Composites Part B 186 (2020) 107828

Contents lists available at ScienceDirect

Composites Part B

journal homepage: www.elsevier.com/locate/compositesb

Nanoparticles of polydopamine for improving mechanical and flame-retardant properties of an epoxy resin

Wenmu Yang [a], Shuying Wu [a,b], Wei Yang [a], Anthony Chun-Yin Yuen [a], Yang Zhou [a], Guan Yeoh [a], Cyrille Boyer [c], Chun H. Wang [a,*]

[a] School of Mechanical and Manufacturing Engineering, University of New South Wales, Sydney, NSW, 2052, Australia
[b] School of Engineering, Macquarie University, Sydney, NSW, 2109, Australia
[c] Centre for Advanced Macromolecular Design, School of Chemical Engineering, High Street, UNSW, Sydney, Australia

ARTICLE INFO

Keywords:
Nanocomposites
Polydopamine
Flammability
Mechanical properties

ABSTRACT

A bio-flame retardant filler was synthesized via the self-polymerization of dopamine hydrochloride in alkaline condition, yielding nano-sized polydopamine (nano-PDA) particles ranging between 50 and 100 nm in diameters. Adding a small amount (2 wt%) of the nano-PDA particles into an epoxy can remarkably reduce the value of peak heat release rate by 53.6%, exceeding the performance aluminum trihydroxide (ATH) particles at 10 wt%. The significant improvement in flame retardancy at a relatively low loading of PDA has been found to originate from several key mechanisms including radical scavenging, higher char yield, and production of CO_2. Furthermore, the addition of nano-PDA in the epoxy resin increased the tensile strength by ~6%. In contrast, the addition of common flame retardant, such as ATH, to achieve the same increase in flame retardancy of epoxy would reduce the tensile strength by 22%. This improvement in mechanical properties is attributed to the better bonding between PDA particles with epoxy than ATH with epoxy.

1. Introduction

Flame retardancy of polymers and fiber reinforced composites commonly used in constructions and lightweight structures, such as polyethylene and epoxy, is emerging as a major safety issue following recent high-profile fire accidents of high-rise buildings that resulted in fatalities [1]. These polymer materials are widely used for their excellent mechanical properties and electrical insulation properties, adhesion to various materials and ease of manufacturing [2]. For instance, epoxy resins are commonly found in the manufacture of plastics, coatings, paints, adhesives, sealants, and lightweight structures used in space craft and aircraft, while polyester and polyethene are commonly used in construction as adhesives, core of metal sandwich, and matrix materials of fiber reinforced composites [3]. In addition, epoxy resins are widely used as the matrix materials of fiber reinforced composites and act as binders to various metal materials and non-metal materials as well as thermosetting plastics. According to the National Fire Protection Association (NFPA) report, there were 1.3 million fires in the United States in 2017, 3400 civilian fire deaths, and 55.4 billion U.S dollars in direct property damage [4]. Related issues and concerns relevant to such statistics emphasize the necessity of improving the flame retardant property of lightweight building materials and home furniture and furnishings [5]. Compared with other commonly used polymers, epoxy resins have poor flame retardant properties [6]. For example, epoxy resin has poor flame retardant properties, and the limit oxygen index of unmodified epoxy resin is only about 19 [7], which means it can continuously burn in air.

The common practice to improve flame retardant performance of polymeric materials is to blend flame retardants, either solid or liquid [8,9]. These flame retardant fillers are categorized by their action modes and come in two classes: 'inert' and 'active'. Inert fillers dilute the combustible mass with incombustible additives and form a char layer that provides thermal insulation and acts as a gas barrier separates fuel from oxygen. Some of the inert fillers also have the effect of absorbing heat due to phase change. Active fillers absorb heat by decomposing at elevated temperatures which could slow the decomposition rate of the polymer matrix, and also produce inert gases such as water vapor, nitrogen and carbon dioxide which diffuse into the flammable volatiles [10]. Active fillers are generally more effective and more widely used than inert fillers in terms of reducing flammability and smoke from

* Corresponding author.
E-mail address: chun.h.wang@unsw.edu.au (C.H. Wang).

https://doi.org/10.1016/j.compositesb.2020.107828
Received 8 August 2019; Received in revised form 17 January 2020; Accepted 29 January 2020
Available online 30 January 2020
1359-8368/

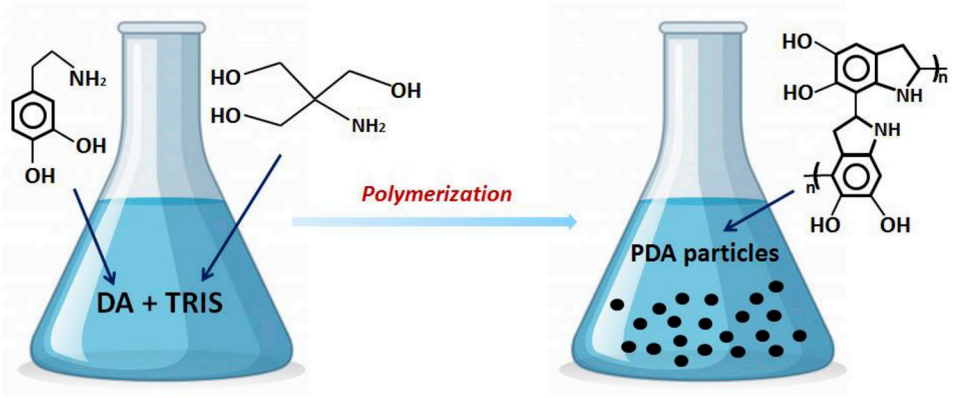

Fig. 1. The chemical structures of the main compounds utilized in this study (TRIS is used to regulate the pH of the solution).

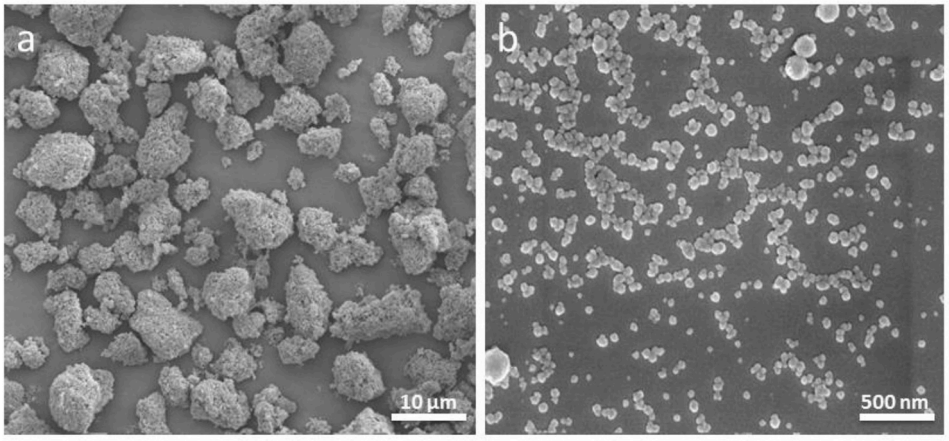

Fig. 2. (a) SEM micrographs of ATHs, and (b) PDAs.

Table 1
Zeta potential values of nano-PDA and ATH particles.

Sample	Average Zeta Potential (mV)
PDA (0.1%) in water	−39.9 ± 3.8
ATH (0.1%) in water	22.7 ± 1.6

polymers. Aluminum trihydroxide (ATH) [11] is a most commonly used active fillers due to their relative low cost and non-toxic gases emissions. However, typically a considerable amount of ATH is needed to improve the flame retardant properties of polymers to meet industry standards. In order to achieve good flame retardant performance, more than 50 wt % of ATH are usually needed which would severely reduce the mechanical and durability properties of polymers [12]. This problem is further exacerbated by the agglomeration/aggregation of ATH particles at this high loading contents, due to the difficulties to achieve uniform dispersion [13].

Recent research [14–16]have found that maximizing the surface area of flame retardant fillers and their bonding with polymers using nanotechnology is a very effective way to simultaneously enhance fire and mechanical properties of polymers. Polydopamine (PDA) [17], a

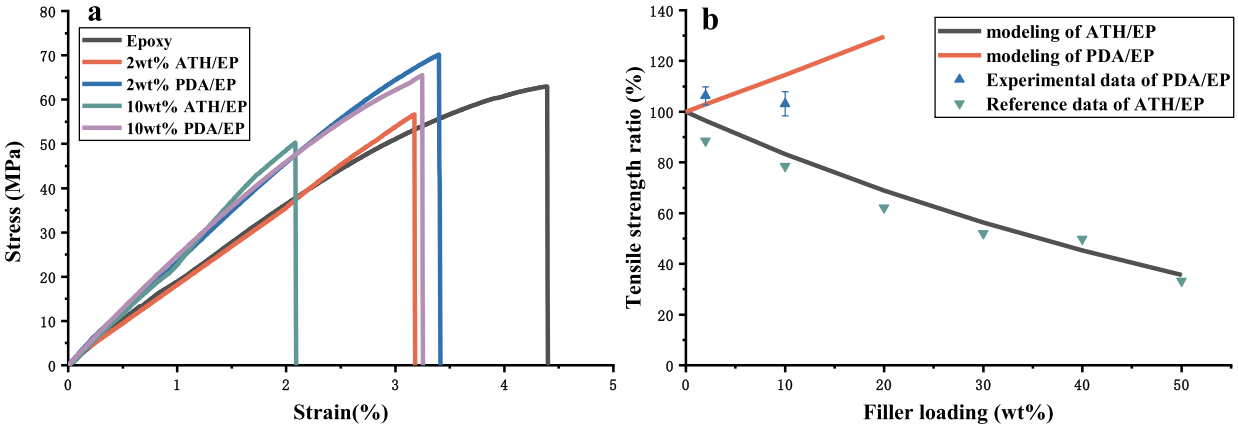

Fig. 3. (a) Typical stress and strain curves of pure epoxy, ATH/EP composites and PDA/EP composites. (b) Predicted tensile strength of different filler loadings.

Table 2
Parameters for Eq (1) and (2).

ρ_E (g/cm^3)	ρ_p (g/cm^3)		σ_E (MPa)	σ_p (MPa)
	ATH	PDA	Epoxy	PDA
1.25	2.42	1.52	64	175

synthetic melanin inspired by the adhesive protein secreted by mussels to give them a remarkable ability to bind themselves strongly to a variety of surfaces. It has been reported that PDA can functionalize a wide range of materials to improve their bonding with polymers [18]. For example, Li et al. [19] reported that PDA-coated carbon nanotubes improved the interfacial interaction between CNTs and epoxy matrix, which led to a significant improvement on the dispersion of CNTs in the epoxy matrix and simultaneous reinforcements in thermal conductivity, thermal stability, and storage modulus by adding CNT@PDA. *Kim* et al. [20] applied a single layer PDA encapsulated coating to empower the alginate capsules the cytoprotective capability. The abilities of better mechanical properties, prevention of gel swelling and UV-C protection have been found on the created core/shell capsules. In addition to the characteristics being nontoxic and environmentally friendly, PDA particles were found to have strong radical scavenging activity [21] which

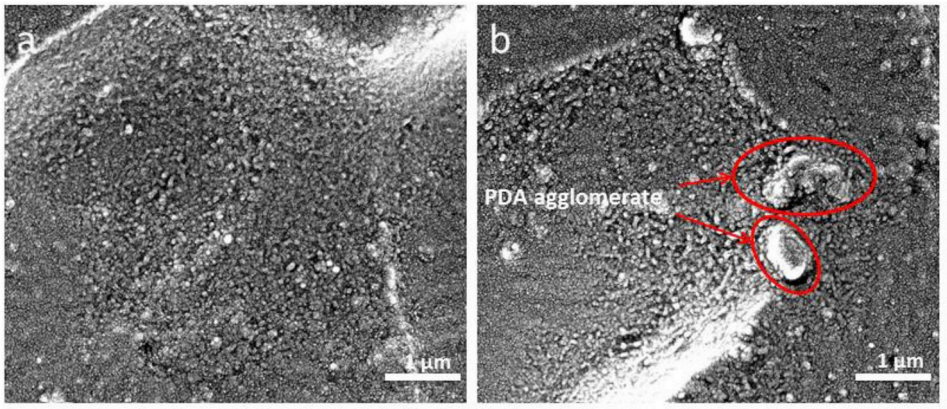

Fig. 4. SEM micrographs of fracture surface of PDA/EP composites with (a) 2 wt% PDAs and (b) 10 wt% PDAs.

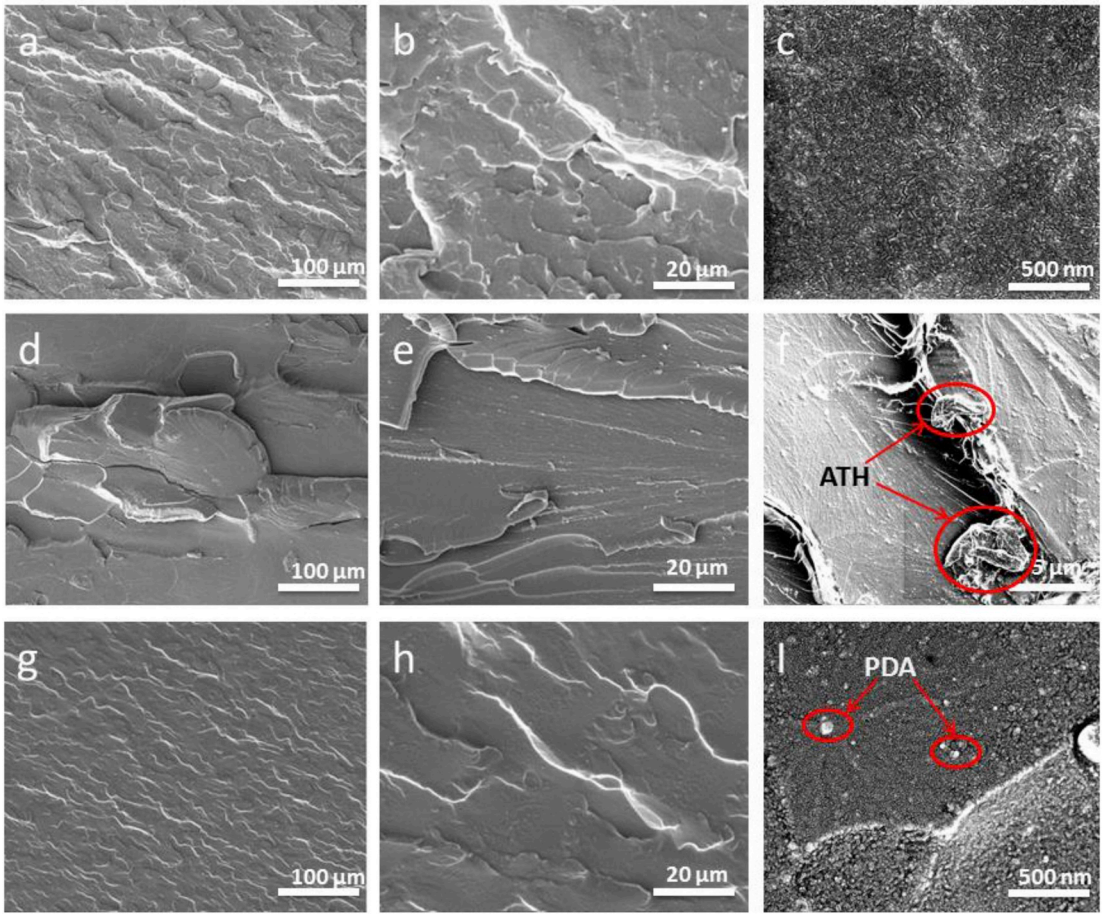

Fig. 5. SEM micrographs of fracture surface of neat epoxy (a,b,c), ATH/EP (d,e,f), and PDA/EP (g,h,i).

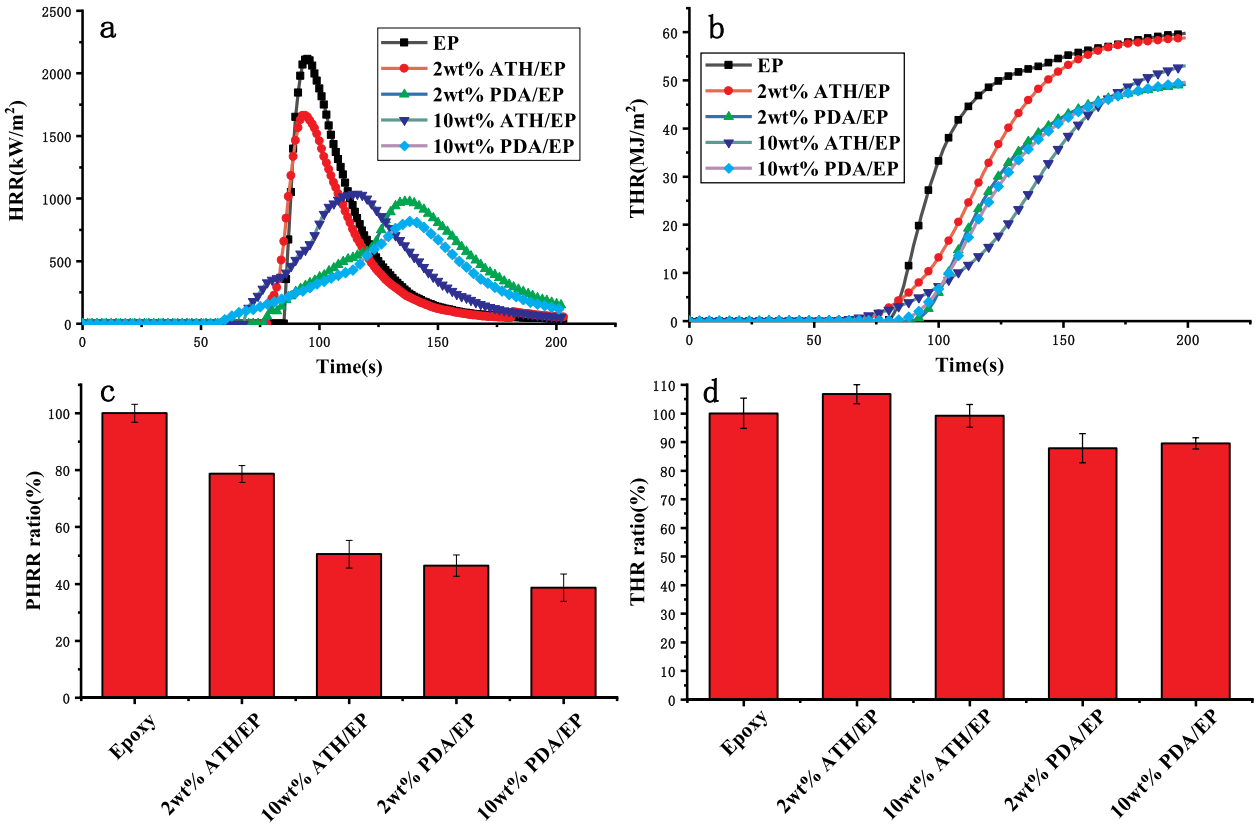

Fig. 6. Fire properties of un-modified and PDA-modified and ATH modified epoxy. (a) Heat release rate, (b) total heat release, (c) peak heat release rate ratio of original epoxy and modified samples (d) total heat release of original epoxy and modified samples.

Table 3
The data of the cone calorimeter results (TTI: time to ignition; PHRR: peak heat release rate; THR: total heat release; TSR: total heat release).

Sample	TTI (s)	PHRR (kW/m^2)	THR (MJ/m^2)	TSR (m [2]/m^2)
EP	36 ± 3	2115 ± 63	60 ± 3	258 ± 21
2 wt% ATH/EP	33 ± 1	1664 ± 25	60 ± 2	1743 ± 91
2 wt% PDA/EP	32 ± 2	982 ± 37	50 ± 2	272 ± 36
10 wt% ATH/EP	28 ± 2	1041 ± 71	56 ± 3	1804 ± 86
10 wt% PDA/EP	26 ± 1	819 ± 56	51 ± 1	341 ± 77

is an important flame retardant ability for highly flammable foamed materials. Cho et al. [22] demonstrated PDA shell as an effective flame retardant coating for flexible polyurethane (PU) foams via a simple dip-coating process.

However, research to date has focused on PDA thin coating, which can only be applied to coat the external surfaces of solids or closed-cell porous materials, or the internal surfaces of open-cell porous materials, such as polyurethane (PU) foam. For surface coating, the fire protection would be easily lost once the fire burns through the coating. Herein we present a new method of simultaneously improving the flame retardancy and mechanical properties of epoxy polymers by dispersing nanosized of PDA particles. Experiments were carried out to characterize the effects of nano-PDA particles on the mechanical properties, thermal stability and flame retardancy in epoxy. The results are compared with the performance of conventional flame retardant ATH.

2. Experimental method

2.1. Materials

Dopamine hydrochloride (DA), tris(hydroxymethyl)aminomethane (TRIS) and aluminum trihydroxide (ATH) were purchased from Sigma Aldrich (AU). The epoxy resin chosen in this study is diglycidyl ether of bisphenol A (DGEBA) and amine curing agent (RAKU TOOL EL-2203/EH-2970) which were supplied by RAMPF Group, Inc. The glass

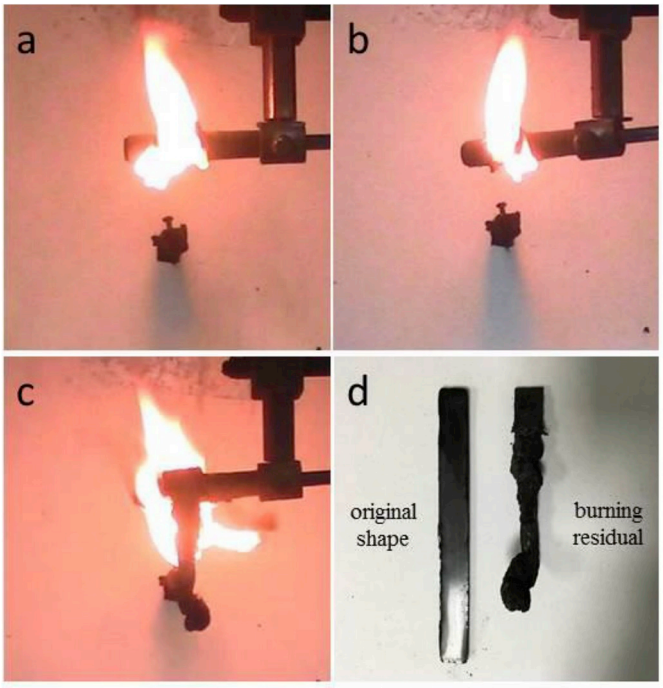

Fig. 7. The ends of combustions of (a) neat epoxy, (b) 2 wt% ATH/EP and (c) 2 wt% PDA/EP, (d) residue of 2 wt% PDA/EP.

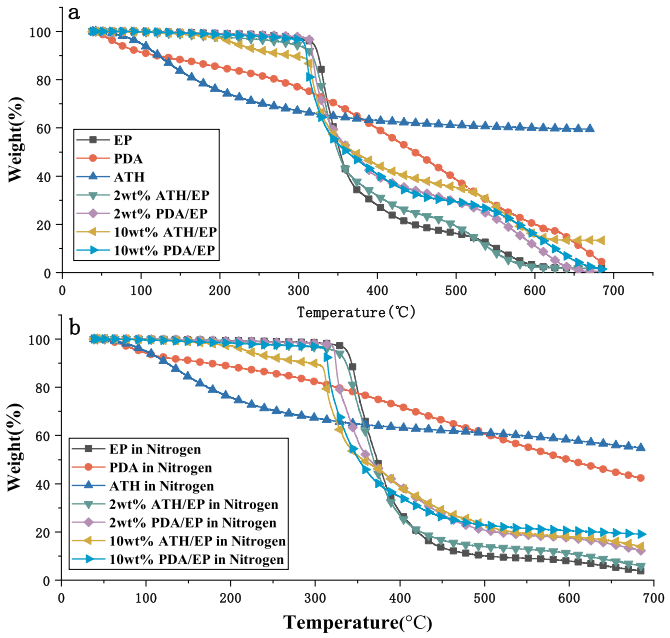

Fig. 8. TGA curves of neat epoxy, ATH/EP and PDA/EP composites in air (a) and nitrogen (b) atmosphere.

Table 4
TGA data for each sample.

Sample	$T_{-5\%}$(°C)		T_{max}(°C)		Residue (wt%) at 700 °C	
	Air	Nitrogen	Air	Nitrogen	Air	Nitrogen
EP	319	337	345	364	1.6	3.6
PDA	70	93	482	498	3.7	42
ATH	100	112	165	178	59.5	54.7
2 wt% ATH/EP	290	323	341	360	1.7	5.7
2 wt% PDA/EP	315	322	343	352	0.6	10.7
10 wt% ATH/EP	219	220	339	332	13.3	13.6
10 wt% PDA/EP	307	312	335	337	1.3	19.1

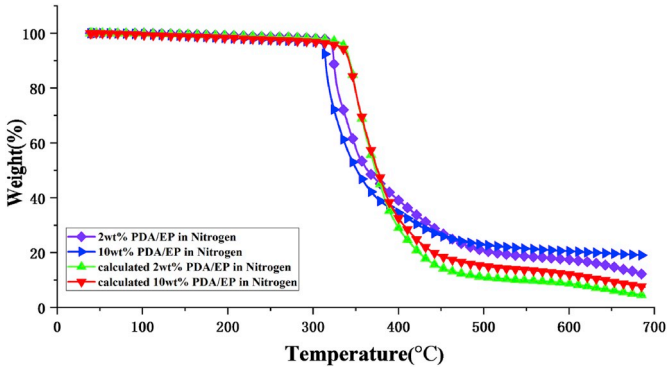

Fig. 9. Comparison of calculated TGA curves and experimental curves for 2 wt % PDA/EP and 10w% PDA/EP in nitrogen atmosphere.

transition temperature of this type of DGEBA is 115–120 °C. The chemical constitutions of the main materials are given in Fig. 1.

2.2. Synthesis of PDA nanoparticles

The synthesis process of PDA is an in-situ polymerization of DA monomers in an alkaline water–ethanol solution at room temperature. The manufacturing process of PDA particles is as follows: 200 mg

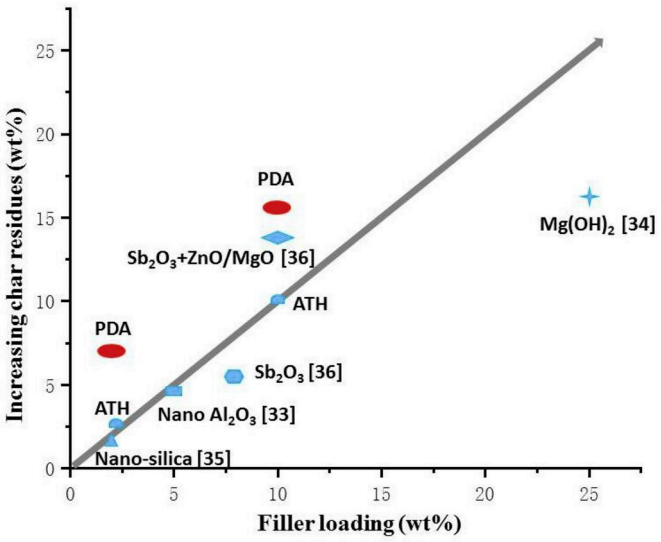

Fig. 10. Char yield of different types of flame retardant fillers [33–36].

dopamine hydrochloride (DA) was dispersed in 10 mM TRIS buffer solution (pH ~ 8.5). The solution was rigorously stirred at room temperature for 3 days [22]. Then the solution was centrifuged, and the supernatant was removed to get concentrated PDA dispersion. PDA particles were then collected by freeze-drying the concentrated dispersion. Fig. 2b shows typical SEM micrographs of the PDA particles. PDA are nano-sized spherical particles with an average particle diameter of 50–100 nm. In contrast, ATH particles are of irregular shape and non-uniform size, as shown in Fig. 2a.

2.3. Manufacturing of flame retardant epoxy composites

Desired amounts (2 wt% and 10 wt%) of PDA and ATH particles were added into the epoxy resin that had been placed in a beaker. Then the mixture was treated by using a Sonics VCX-750 Vibra Cell Ultra Sonic Processor (40% amplitude; pulse duration: 5 s ON, 5 s OFF) under an ice water condition for 1 h. Subsequently, hardener (amine) and DGEBA were mixed in the proportion of 100:25 by weight. . All components were rigorously mixed together at room temperature and degassed for 20 min. Finally, the mixture was poured into a custom-made mold. All samples were cured at room temperature for 24 h.

2.4. Characterizations

Thermal gravimetric analysis (TGA) was performed on a Perkin Elmer (STA6000). Scanning electron microscopy (SEM) was employed to observe the microscopic morphology of particles and the cross-section of the composites. Cone calorimetry (FTT iCone Classic) was conducted to measure the peak heat release rate (PHRR) and total heat rate (THR) of the pure epoxy and epoxy with PDA or ATH fillers at a radiation flux of 50 kW/m^2 (according to ISO 5660–1).; the data could be used to predict the behavior of polymeric materials under large scale fires [23]. Parameters such as heat release rate (HRR), total heat release (THR), and gas emissions are very important during the combustion. The gas flow rate and oxygen consumption rate jointly determine the HRR value. Peak heat release rate (PHRR) is the highest point in the HRR/time plot which is regarded as the most significant parameter to assess the flammability of a material. The area enclosed by the HRR curve and the time axis is THR. Flammability was measured using the Vertical burning test (UL94). Fourier transform infrared spectroscopy (FTIR) was performed to analyze the escape gases during TGA test and the composition of char residuals after cone calorimeter test. Raman spectra were obtained from an Invia Raman spectrometer (532, 633, 785, 830 nm) in the

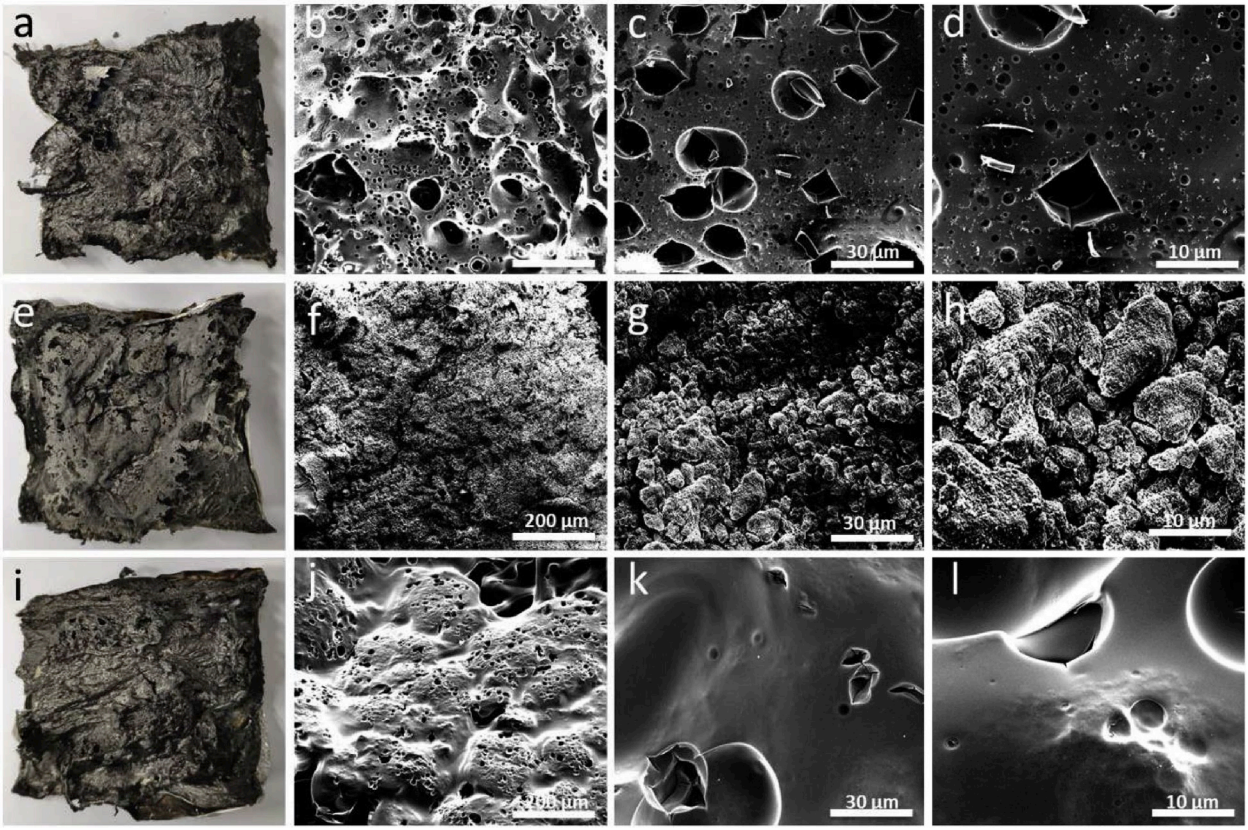

Fig. 11. Residues after cone calorimeter tests: (a–d) neat epoxy, (e–h), 2 wt% ATH/EP, and (i–l) 2 wt% PDA/EP.

Table 5
The parameters of the curve fitting model.

model	Gauss					
equation	$y = y_{0D} + \frac{A_D}{w_D * s \ \ qrt(pi/2)} * \exp\left(-2 * \frac{x - x_{cD}}{w_D}\right)^2 + y_{0G} + \frac{A_G}{w_G * s \ \ qrt(pi/2)} * \exp\left(-2 * \frac{x - x_{cG}}{w_G}\right)^2$					
Sample	EP residues		2 wt% ATH/EP residues		2 wt% PDA/EP residues	
	D Peak	G peak	D Peak	G peak	D Peak	G peak
y_0 (offset)	111,588 ± 422	111,588 ± 422	110,604 ± 578	110,604 ± 578	2637 ± 74	2637 ± 74
x_c (center)	1356.7 ± 0.9	1581.7 ± 0.4	1353.5 ± 1.2	1582.7 ± 0.6	1338.6 ± 0.3	1571.4 ± 0.2
w (width)	272.5 ± 1.9	92.4 ± 1.0	263.6 ± 2.7	96.3 ± 1.4	172.9 ± 0.6	106.9 ± 0.4
A (area)	1.0E8 ± 713,793	3.0E7 ± 468,604	1.1E8 ± 978,812	3.4E7± 683,608	2.3E7 ± 73,113	1.5E7 ± 56,908

wavenumber range from 500 to 2000 cm^{-1}. Tensile tests were conducted on an Instron tensile machine (Instron 3369).

3. Results and discussion

3.1. Dispersion properties of PDA and ATH particles

When particles are dispersed in a solvent, charged particles attract oppositely charged particles in the dispersion. Ions near the surface of the particle are strongly bound while those farther away the surface forms a loose electron cloud. A measure of the internal and external potential difference of the electron cloud is the Zeta potential. The higher the zeta potential magnitude (positive or negative), the more stable is the colloidal system (i.e., the dissolution or dispersion could resist aggregation). Conversely, the lower the zeta potential magnitude, the more prone is for the particles to coagulate or agglomerate. Zeta potential was characterized using the electrophoresis method where particles were kept in diluted deionized water with the pH value of 7.5. According to the zeta potential value of PDA and ATH particles listed in Table 1, PDA can form a more stable dispersibility than ATH particles in water.

3.2. Tensile properties of epoxy composites

Typical tensile test results for each type are shown in Fig. 3a. It can be seen that, by adding ATH, the tensile properties of the composites significantly decrease, as presented in Fig. 3a. For example, the addition of only 2 wt% ATH caused the tensile strength of the epoxy to decrease by about 13% from 64 to 56 MPa, referring to Fig. 3b. By contrast, the tensile strength of epoxy is improved by about 6.25% from 64 to 68 MPa with 2 wt% PDA additives. At 10 wt%, ATH reduced the epoxy strength by 22% while PDA particles did not cause any reduction in strength (the epoxy with 10 wt% PDA retained the same strength as the un-modified epoxy).

The effects of ATH and PDA particles on the mechanical strength of the composite can be estimated by following equations [24]:

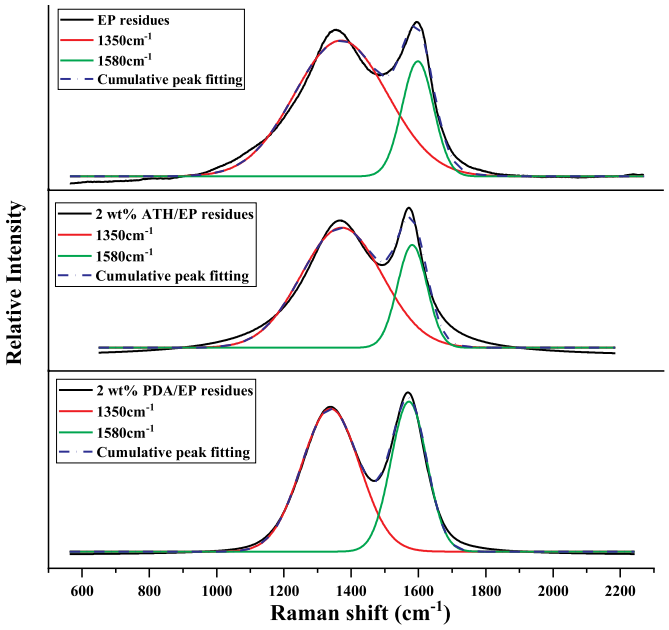

Fig. 12. Raman spectra of the residues for EP, ATH/EP and PDA/EP.

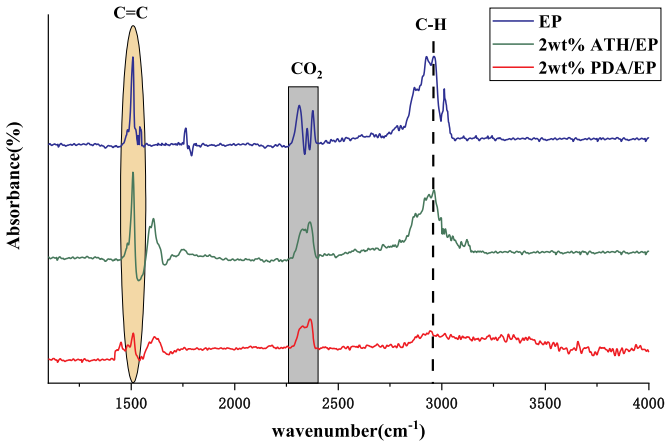

Fig. 13. FTIR spectra of evolved gas during TG process of neat epoxy, ATH/EP and PDA/EP at 485 °C.

Table 6
Characteristic attribution of FTIR absorption bands.

Band position (cm^{-1})	Assignment
2930	C–H
2364	CO_2
1508	C=C

$$\frac{\sigma_{poor-bonding}}{\sigma_E} = \frac{1 - V_f}{1 + 2.5V_f} \quad (1)$$

$$\frac{\sigma_{good-bonding}}{\sigma_E} = \frac{V_f \sigma_f}{\sigma_E} + (1 - V_f) \quad (2)$$

where V_f is filler volume fraction, σ_f and σ_E are the tensile strength of the filler and the epoxy matrix strength, respectively. Eq (1) is based on the hypothesis that there is no bonding force between filler (ATH) and matrix, and the stress cannot be transferred between the matrix and the filler. Eq (2) is for the pattern of very strong interfacial bonding (PDA/EP) so the bonding strength between the fillers and the matrix is greater

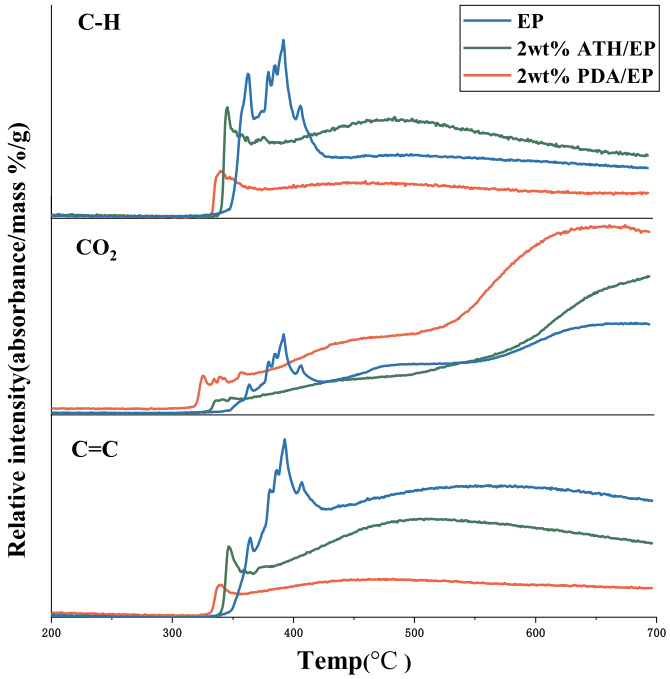

Fig. 14. The change trends of 3 main signals with temperature.

than the composite strength. The filler volume fraction V_f can be determined from the weight percentage:

$$\frac{\rho_f V_f}{\rho_E (1 - V_f)} = \frac{Weight\%}{1 - Weight\%} \quad (3)$$

where ρ_E and ρ_f are the density of epoxy matrix and the fillers. Parameters have been calculated and shown in Table 2. The density of epoxy matrix ρ_E is 1.25 g/cm^3 [25,26], and the density for ATH and PDA particles (ρ_f) are 2.42 g/cm^3 [27] and 1.52 g/cm^3 [28] respectively. The tensile strength of PDA (σ_f) is about 175 MPa [29] and the calculated value of σ_{ATH} and σ_{PDA} are shown in Fig. 3b.

According to the comparison of experimental data and modelling data in Fig. 3b [30], PDA (2 wt%)/epoxy composites showed the highest tensile strength. As the loading of the PDAs increases to 10 wt%, the strength enhancement became less noticeable (different with the modeling trend), which is probably due to the agglomeration of PDAs at this high loading that causes localized stress concentrations, as indicated by Fig. 4b.

The fracture surfaces of the epoxy composites were examined by SEM. Fig. 5 shows the SEM micrographs of neat epoxy and epoxy composites. The fracture surface of pure epoxy resin showed a smooth surface, as shown in Fig. 5a, which are typical of brittle fracture. The fracture surfaces of the epoxy containing ATH particles (Fig. 5f) are rough and debonding is clearly visible at the interface between ATH particles and epoxy matrix. Poor interface bonding and dispersion of ATH affect the mechanical properties of the composites. From Fig. 5i, the fracture surface of epoxy-PDA composites shows that PDAs are uniformly distributed and embedded in epoxy matrix and well bonded with epoxy without any sign of interface debonding. This difference between ATH and PDA particles is attributed to the presence of amines and catechol functional groups on the PDA surface allowing reactions with epoxy groups and enhancing interface interaction between PDA and epoxy [19]. Consequently, the stress would transfer from the low modulus (polymer matrix) to the high modulus [31] (PDA fillers) effectively, thus increasing the tensile strength with relatively low PDAs loading. Besides, due to the presence of the hydroxyl and amine groups of PDA, which participate in the curing process of epoxy, PDA also has better chemical compatibility with epoxy [32].

3.3. Fire behaviors of the epoxy composites

3.3.1. Cone calorimeter test

Fig. 6 presents the results of heat release rate (HRR) and total heat release (THR) as a function of burning time for the un-modified epoxy and the samples containing 2 wt% and 10 wt% of PDA nanoparticles and ATH particles. The relevant data have been summarized in Table 3. Neat epoxy exhibited a peak heat release rate (PHRR) of 2115 kW/m^2 and a total heat release (THR) of 56.5 MJ/m^2. Compared to ATH/EP and neat epoxy, the addition of 2–10 wt% of PDAs resulted in a significant reduction in the PHRR and THR data. The PHRR and THR reductions for the four configurations are plotted in Fig. 6c and d. It is clear that adding 2 wt% of nano-PDA particles led to a remarkable reduction in the PHRR data by 53.6% and 12% reduction in the THR compared with neat epoxy. When the loading of nano-PDA particles was increased to 10 wt %, the reduction in PHRR reached 60.3% and the THR reduction did not increase any further. By contrast, the addition of 2 wt% of ATH to epoxy only yielded a slight reduction in the PHRR and an increase in the THR. The effectiveness of 2 wt% nano-PDA particles far exceeds that of ATH of the same load and is better than 10 wt% of ATH particles. In addition, the time to reach peak heat release rate has also been delayed by the incorporation of nano-PDA particles.

3.3.2. UL94 test

Results of UL94 tests show little difference in the flame retardant levels, mainly due to the low concentrations of the fillers. However, the char residuals displayed in Fig. 7 show significant differences: epoxy with PDA fillers yielded significantly more residue, which resembles the general shape of the sample after burning. This is in stark contrast with neat epoxy and epoxy with ATHs where no residual was left after the UL94 tests.

3.4. Flame retarding mechanisms

Recent research has identified two major flame retardant mechanisms for PDA surface coating [22]: (i) a char forming ability, (ii) the catechol units to scavenge nearby radicals to reduce fuel for fire. The char forming ability is evidenced by the weight of the TGA residues, char layer morphology, and the carbonization degree of the residues after cone calorimeter tests. The radical scavenging property could be confirmed by analyzing the functional groups of gases escaping during TGA-FTIR test.

3.4.1. Char forming ability

Fig. 8 shows the thermal decomposition of neat epoxy resin, ATH/EP and PDA/EP composites under air and nitrogen atmosphere, and the corresponding TGA data are summarized in Table 4. The temperature of 5 wt% mass loss ($T_{-5\%}$) is often treated as the start of decomposition. When PDAs were added to the epoxy, the $T_{-5\%}$ decreased slightly from 337 °C to 322 °C, indicating that PDAs started decomposing before the epoxy. Moreover, the temperature of maximum degradation rate (T_{max}) decreased from 364 °C to 322 °C. However, the weight of char residues increased from 3.6 wt% to 10.7 wt% for 2 wt% PDA additives, 19.1 wt% for 10 wt% PDA additives. The increasing char residues indicating that the decomposition products of PDAs have considerably improved the char yield of epoxy during the pyrolytic process.

Fig. 9 indicates the calculated TGA curves and experimental data for 2 wt% and 10 wt% PDA additives. The calculated data (M_L) is obtained by the following equation:

$$M_L = V_m D_m + V_f D_f$$

where V_m and V_f are weight percentage of matrix and fillers, D_m and D_f are the TGA data of neat matrix and pure fillers. Therefore, if there is no interaction phenomenon between the matrix and fillers, the linear sum curve should be the same with the experimental values of M_L. However, a comparison between the experimental results and the liner model prediction reveals that the actual char residue after thermal decomposition is about three times the predicted value by the linear model. This provides an evidence of the synergistic interaction between PDA and epoxy that led a better char forming process.

For comparison purpose, the increase in char yield ratio (S) due to the addition of flame retardant fillers, defined as the difference between the char yield ratio of the composite (R_c) and the char yield ratio of the matrix (R_m),

$$S = R_c - (1 - V_f)R_m \tag{4}$$

Where R denotes the char yield ratio defined as the ratio of char to the original weight of the test sample, with the subscripts c and m denoting the composite and the matrix. In the case of fillers that do not increase char yield, we have $R_c = V_f + (1 - V_f)R_m$, so the value of S will be equal to the filler content V_f. Therefore, if the value of S exceeds V_f, it would indicate a synergistic effect between the filler and the matrix in char formation. A comparison of the effect of PDA particles on char yield with other commercial flame retardant fillers reported in the literature [33–35], including ATH, is shown in Fig. 10. For these common flame-retardant fillers, the resultant increases in char yield ratios are equal to or less than weight percentage of the fillers, indicating the lack of synergistic effect. It is clear from the comparison shown in Fig. 10 that nano-PDA particles generate significantly a higher char yield ratio than common commercially flame retardant fillers. In particular, at both 2 wt % and 10 wt%, nano-PDA particles outperform the best result by Sb_2O_3+ZnO/MgO reported in the literature [36].

The above results are consistent and supported by the high-density chars of epoxy containing nano-PDA particles. Optical images and SEM micrographs of cone tested residual chars are shown in Fig. 11. Obviously, the char of neat epoxy is loose and porous, shown as Fig. 11a–d. Samples containing ATHs particles showed a thin white shell structure [37]. This structure is formed by metal oxide particles (Fig. 11e); some of which may be from the soot product of the gas-phase combustion. A low-density porous structure is highly permeable and allows the transport of fuel and oxygen between the flame and composite. The SEM micrographs of the char of PDA-enhanced epoxy show a dense, solid carbon layer which hinders the mass and oxygen transfer, thereby effectively interrupting the combustion cycle.

To further ascertain the flame retardant mechanisms, Raman spectroscopy was used to quantify the degree of graphitization of the carbon materials in the combustion residues [38]. Carbon with higher graphitization degree is usually associated with higher resistance to thermal oxidation or higher flame retardancy. The Raman spectra of pure epoxy and PDAs/EP composites reveal two peaks at around 1350 cm^{-1} and 1580 cm^{-1}, respectively named the D band and G band. The area ratio of the D and G bands (I_D/I_G) [39] indicates the graphitization degree of carbonaceous materials. The higher the I_D/I_G value, the lower the degree of graphitization [40]. The D and G peak positions were determined by a Gauss fit after baseline subtraction [41]. The parameters of the curve fitting model are shown in Table 5. The I_D/I_G value of char residue for pure epoxy and ATH/EP is 3.48 and 3.09 respectively, while the value of I_D/I_G is reduced to 1.52 of the PDA/EP sample shown in Fig. 12. The result indicates that the PDA particles increased the graphitic phases in char which provides more effective barriers against mass and heat diffusion.

3.4.2. Radical scavenging property

TG-IR technique was used to analyze the gas products during the thermal degradation process which can help understand the mechanism of the thermal decomposition. Normalized FTIR spectra of evolved gas during TG process of different samples at 485 °C are shown in Fig. 13. Three representative gas products of the epoxy composites are identified by the characteristic strong FTIR signals, as shown in Table 6. The peaks at about 2930 cm^{-1} indicate the appearance of the stretching vibrations

of C–H [42]. The asymmetric peaks at 2364 cm^{-1} indicate the presence of CO_2 [43]. The peak around 1508 cm^{-1} is attributed to C═C stretching vibrations [44].

In order to characterize the effects of PDA nanoparticles and ATH particles on volatilized gas products (C–H, CO_2, and C═C), the three pertinent signals of the gas-phase spectra with time are extracted from the original data and shown in Fig. 14. It is seen that the pyrolysis products for ATHs/EP and PDAs/EP occurs slightly earlier than neat epoxy which is consistent with the TGA and cone calorimeter results shown in Fig. 6a. From Fig. 14, the C–H and C═C break down earlier than epoxy during the heating process, but the presence of PDA has reduced the peak intensities to be lower than those for pure epoxy and ATHs/EP. Since the C–H and C═C are combustible gases which could provide additional fuel for the fire, their reduction is another evidence that PDA is capable of radical scavenging. Furthermore, the captured C═C is a source of the char residues. Therefore, the reason why PDA-modified epoxy has better char forming property is that PDA can capture free carbon released during the combustion process and generate more char residues.

3.4.3. Volatilized gas products

In addition, the results in Fig. 14 show that PDA nanoparticles also increase the CO_2 production at temperatures above 400 °C. The addition of PDA suppressed C–H and C═C, therefore, the carbon from C–H turn to form more CO_2 which have been released. CO_2 is an effective barrier that can reduce the oxygen available to the fuel and heat conduction during the combustion process. So the formation of denser char, radial scavenging, production of CO_2 are some of the key mechanisms contributing to the increased flame retardancy in PDA enhanced epoxy (as indicated by the lowest HRR and THR from the cone calorimeter test).

4. Conclusion

Nano-sized polydopamine particles, synthesized via a self-polymerization of dopamine hydrochloride in alkaline condition, has been found to significantly improves the flame retardancy of epoxy polymer even at relatively low concentration. In particular, adding 2 wt % PDA nanoparticles can lower the peak heat release rate and the total heat release by 53.6% and 12%, respectively, significantly better than what could be achieved by aluminum trihydroxide particles of the same weight loading. Through detailed analysis of the char morphology, graphitic content, and gas-phase combustion products, the key mechanisms responsible for these improvements have been identified as increased char density, radial scavenging, and production of CO_2. Analyses of the PDA flame retardant mechanism have highlighted the synergistic effect of barrier effect and radicals scavenging effect on overall the flame retardant efficiency of a material system. PDA nanoparticles are effective in forming a char of a higher density than the epoxy with commercial flame retardant fillers, which restrict heat conduction and the transport of oxygen, fuel, and volatile groups. In addition, PDA nano-particles act as an effective mechanical reinforcement to improve of strength for epoxy composites. The increase in tensile strength is attributed to the good dispersion of PDA nanoparticles and their cross-linking with the epoxy matrix. The nano-PDA particles offer a new method of improving epoxy polymers and their fiber-reinforced composites.

CRediT authorship contribution statement

Wenmu Yang: Methodology, Validation, Formal analysis, Investigation, Writing - original draft. **Shuying Wu:** Conceptualization, Supervision. **Wei Yang:** Methodology. **Anthony Chun-Yin Yuen:** Resources. **Yang Zhou:** Formal analysis. **Guan Yeoh:** Conceptualization. **Cyrille Boyer:** Resources. **Chun H. Wang:** Conceptualization, Writing - review & editing, Supervision, Project administration.

Acknowledgment

This work was financially supported by Australian Research Council Industrial Transformation Training Center (ARC IC170100032) in the University of New South Wales. The author S. Wu would like to thank the Australia Research Council for financial support through Discovery Early Career Researcher Award (DE170100284).

Appendix A. Supplementary data

Supplementary data to this article can be found online at https://doi.org/10.1016/j.compositesb.2020.107828.

References

[1] Wicklein B, et al. Thermally insulating and fire-retardant lightweight anisotropic foams based on nanocellulose and graphene oxide. Nat Nanotechnol 2015;10(3):277.
[2] Gu H, et al. An overview of multifunctional epoxy nanocomposites. J Mater Chem C 2016;4(25):5890–906.
[3] Unnikrishnan K, Thachil ET. Toughening of epoxy resins. Des Monomers Polym 2006;9(2):129–52.
[4] Zhuang J, et al. Total cost of fire in the United States. Fire Protection Research Foundation; 2017.
[5] Karter MJ. Fire loss in the United States during 2003. MA: National Fire Protection Association Quincy; 2004.
[6] Liu S, et al. A review of extending performance of epoxy resins using carbon nanomaterials. Compos B Eng 2018;136:197–214.
[7] Liu YL. Flame-retardant epoxy resins from novel phosphorus-containing novolac. Polymer 2001;42(8):3445–54.
[8] Le Bras M, Wilkie CA, Bourbigot S. General considerations on the use of fillers and nanocomposites. In: An introduction to the use of fillers and nanocomposites in fire retardancy; 2007. p. 1–14.
[9] Feng Y, et al. Improving thermal and flame retardant properties of epoxy resin by functionalized graphene containing phosphorous, nitrogen and silicon elements. Compos Appl Sci Manuf 2017;103:74–83.
[10] Yang H, et al. Surface-coating engineering for flame retardant flexible polyurethane foams: a critical review. Compos B Eng 2019;176:107185.
[11] Nelson G, Wilkie CA. Fire and polymers(materials and solutions for hazard prevention). In: A. C. S. symposium series. American Chemical Society; 2001.
[12] Weil ED, Levchik S. A review of current flame retardant systems for epoxy resins. J Fire Sci 2004;22(1):25–40.
[13] Qin Z, et al. Effect of nano-aluminum hydroxide on mechanical properties, flame retardancy and combustion behavior of intumescent flame retarded polypropylene. Mater Des 2016;89:988–95.
[14] Fang F, et al. Improved flame resistance and thermo-mechanical properties of epoxy resin nanocomposites from functionalized graphene oxide via self-assembly in water. Compos B Eng 2019;165:406–16.
[15] Fang F, et al. A facile way to prepare phosphorus-nitrogen-functionalized graphene oxide for enhancing the flame retardancy of epoxy resin. Compos Commun 2018;10:97–102.
[16] Zhang L, et al. Polydopamine induced natural fiber surface functionalization: a way towards flame retardancy of flax/poly (lactic acid) biocomposites. Compos B Eng 2018;154:56–63.
[17] Liu M, et al. Recent developments in polydopamine: an emerging soft matter for surface modification and biomedical applications. Nanoscale 2016;8(38):16819–40.
[18] Jia X, et al. Adhesive polydopamine coated avermectin microcapsules for prolonging foliar pesticide retention. ACS Appl Mater Interfaces 2014;6(22):19552–8.
[19] Ling Y, et al. Epoxy resin reinforced with nanothin polydopamine-coated carbon nanotubes: a study of the interfacial polymer layer thickness. RSC Adv 2016;6(37):31037–45.
[20] Kim BJ, et al. Cytoprotective alginate/polydopamine core/shell microcapsules in microbial encapsulation. Angew Chem Int Ed 2014;53(52):14443–6.
[21] Ju K-Y, et al. Bioinspired polymerization of dopamine to generate melanin-like nanoparticles having an excellent free-radical-scavenging property. Biomacromolecules 2011;12(3):625–32.
[22] Cho JH, et al. Bioinspired catecholic flame retardant nanocoating for flexible polyurethane foams. Chem Mater 2015;27(19):6784–90.
[23] Yang W, et al. Manufacturing, mechanical and flame retardant properties of poly (lactic acid) biocomposites based on calcium magnesium phytate and carbon nanotubes. Compos Appl Sci Manuf 2018;110:227–36.
[24] Fu S-Y, et al. Effects of particle size, particle/matrix interface adhesion and particle loading on mechanical properties of particulate–polymer composites. Compos B Eng 2008;39(6):933–61.
[25] Thompson ZJ, et al. Block copolymer toughened epoxy: role of cross-link density. Macromolecules 2009;42(7):2333–5.
[26] Xu Z, et al. Epoxy nanocomposites simultaneously strengthened and toughened by hybridization with graphene oxide and block ionomer. Compos Sci Technol 2018;168:363–70.

[27] Bee ST, et al. Effects of irradiation on the mechanical, electrical, and flammability properties of (low-density polyethylene)/(ethylene-[vinyl acetate] copolymer) blends containing alumina trihydrate. J Vinyl Addit Technol 2014;20(2):91–8.
[28] Nishizawa N, et al. Polydopamine particle as a particulate emulsifier. Polymers 2016;8(3):62.
[29] Lin S, et al. Tuning heterogeneous poly (dopamine) structures and mechanics: in silico covalent cross-linking and thin film nanoindentation. Soft Matter 2014;10(3):457–64.
[30] Fuzail M, Shah G, Anwar J. Modification of polyethylene and incorporation of Al (OH) 3 for improvement of mechanical properties, burning behaviour and thermal stability. Iran Polym J (Engl Ed) 2010;19:47–56.
[31] Fei B, et al. Coating carbon nanotubes by spontaneous oxidative polymerization of dopamine. Carbon 2008;46(13):1795–7.
[32] Chen S, Cao Y, Feng J. Polydopamine as an efficient and robust platform to functionalize carbon fiber for high-performance polymer composites. ACS Appl Mater Interfaces 2013;6(1):349–56.
[33] Jin F-L, Park S-J. Thermal properties of epoxy resin/filler hybrid composites. Polym Degrad Stabil 2012;97(11):2148–53.
[34] Baggaley R, et al. The influence of novel zinc hydroxystannate-coated fillers on the fire properties of flexible PVC. Fire Mater 1997;21(4):179–85.
[35] Rusu G, Rusu E. Nylon 6/SiO2Nanocomposites synthesized by in situAnionic polymerization. High Perform Polym 2006;18(3):355–75.
[36] Tian C, et al. Flame retardant flexible poly (vinyl chloride) compound for cable application. J Appl Polym Sci 2003;89(11):3137–42.
[37] Zammarano M, et al. Preparation and flame resistance properties of revolutionary self-extinguishing epoxy nanocomposites based on layered double hydroxides. Polymer 2005;46(22):9314–28.
[38] Yu B, et al. Interface decoration of exfoliated MXene ultra-thin nanosheets for fire and smoke suppressions of thermoplastic polyurethane elastomer. J Hazard Mater 2019;374:110–9.
[39] Zhang L, et al. Ambient NH 3 synthesis via electrochemical reduction of N 2 over cubic sub-micron SnO 2 particles. Chem Commun 2018;54(92):12966–9.
[40] Carosio F, et al. Graphene oxide exoskeleton to produce self-extinguishing, nonignitable, and flame resistant flexible foams: a mechanically tough alternative to inorganic aerogels. Adv Mater Interfaces 2018;5(23):1801288.
[41] Sadezky A, et al. Raman microspectroscopy of soot and related carbonaceous materials: spectral analysis and structural information. Carbon 2005;43(8):1731–42.
[42] Wang X, et al. Thermal degradation mechanism of flame retarded epoxy resins with a DOPO-substitued organophosphorus oligomer by TG-FTIR and DP-MS. J Anal Appl Pyrol 2011;92(1):164–70.
[43] Braun U, et al. Influence of the oxidation state of phosphorus on the decomposition and fire behaviour of flame-retarded epoxy resin composites. Polymer 2006;47(26):8495–508.
[44] González MG, Cabanelas JC, Baselga J. Applications of FTIR on epoxy resins-identification, monitoring the curing process, phase separation and water uptake. In: Infrared spectroscopy-materials science, engineering and technology. IntechOpen; 2012.